Thermal Properties of Mn-doped LiNbO₃ Crystals from Magneto-Optical Transitions

Jung-Il Park*

Nano-Physics and Technology Laboratory, School of Physics and Energy Sciences, Kyungpook National University, Daegu 702-701, Korea

In this study, we determine that the electron paramagnetic resonance line-width (EPRLW) is axially symmetric about the c-axis and analyze the spin Hamiltonian with an isotopic g-factor of 1.9920 at a frequency of 9.5 GHz. It should be noted that the electron paramagnetic resonance signals are Lorentzian. Our findings show that the EPRLW decreases exponentially with an increase in the temperature; i.e., its temperature dependence in the range 300-400 K obeys Arrhenius behavior, this kind of temperature dependence indicates an off-center a motional narrowing of the spectrum when Mn^{2+} impurity ions substitute for Nb^{5+} ions. The specific heats follow a linear dependence suggesting a simple Debye T^3 behavior.

Keywords : electron paramagnetic resonance line-width (EPRLW), projection-isolation technique (PIT), magneto-optical transition, specific heat

1. Introduction

Electron paramagnetic resonance (EPR) spectroscopy is a technique based on microwave absorption by electrons with unpaired spins in the presence of external electromagnetic radiation. Extensive experimental and theoretical work has been conducted with the objective of generating an electron paramagnetic resonance line-profile (EPRLP) and an electron paramagnetic resonance line-width (EPRLW) for ferroelectric single crystals in a circularly polarized radiation field. Paramagnetic ions, including those of the transition metals $3d^3(Cr^{3+}, V^{2+})$, $3d^4(Mn^{3+}, Cr^{2+})$, $3d^5(Fe^{3+}, Mn^{2+})$, $3d^6(Fe^{2+})$, and $3d^9(Cu^{2+})$, and rare earth elements, belong to the most important type of impurities in lithium niobate, $LiNbO_3$ (LNO) [1, 2]. LNO has found use in ultrasonic transducers [3], electro-optic modulators, surface acoustic wave devices, etc. [4-6]. Doped LNO crystals have found use in holographic storage and laser hosting. EPR studies on Mn-doped LNO crystals have been reported by several authors: Taketa *et al.* [7], Petrov [8], and Rexford *et al.* [9]. In addition to these EPR studies, many other experiments involving nuclear magnetic resonance (NMR), nuclear quadrupole resonance (NQR), the Mössbauer effect, optical absorption, and magnetic properties have been performed.

From a theoretical point of view, the studies performed so far on a resonant system in the presence of external electromagnetic radiation have usually been based on the following methodologies: the Boltzmann transport theory, Green's function approach, the force-balance approach, Feynmann's path integral approach [10], and the projection operator technique [11]. There have been numerous techniques for the calculation of resonance line-widths. Using the density operator method, Arora and Spector obtained a formula for various resonant systems including acoustic phonons. Suzuki [12] presented a formula for electron systems using the resolvent superoperator method. Peeters and Devreese [13] presented a theory using the memory function method and applied it to study various two- and three-dimensional electron systems. Shibata and Ezaki developed a new type of expansion technique for determining time-correlation function, obtained kinetic coefficients using Mori's projection method [11]. This technique is applied for studying magnetic impurity systems. Among the above mentioned techniques, we focus on the projection-isolation technique (PIT) approach of Argyres and Sigel [14]. The projection operator in the theory of Argyres and Sigel contains the electron spin index. By using this method, we succeeded in formulating a response theory [15, 16], which includes the Kubo theory as the effective lowest-order approximation [17, 18]. The EPRLP function derived is similar to those obtained by other methods [10,

*Corresponding author: Tel: +82-53-950-5316
Fax: +82-53-952-1739, e-mail: jipark@knu.ac.kr

11]. Furthermore, the amount of calculation steps involved in the technique of Argyres and Sigel is considerably lesser than that required for any other technique.

In this study, we first use the partition function to calculate the specific heat of LNO crystals that have been Mn-doped at 0.5 wt%. Next, the EPRLW is obtained using the PIT developed by Argyres and Sigel and compared with the experimental data of Ellabban *et al.* [19]. We expand the EPRLP scattering strength term using a series expansion. On the basis of the numerical calculations, we analyze the absorption power for magneto-optical quantum transitions and the temperature dependence of the EPRLW at a frequency of 9.5 GHz in the presence of external electromagnetic radiation. Finally, we discuss our analysis and draw conclusions.

2. System

In the ferroelectric phase a LNO crystal exhibits a three-fold rotation symmetry about its *c*-axis. Thus, it is a member of the trigonal crystal system. In addition, it exhibits mirror symmetry about three planes that are 60° apart and intersect with each other, forming a three-fold rotation axis. These two symmetries classify LNO as a member of the 3*m* point group. It also belongs to the *R3c* space group. In the trigonal system, two different unit cells can be chosen, either hexagonal or rhombohedral. We select the hexagonal unit cell for studying the crystal structure of LNO in its ferroelectric phase.

For an external polarized radiation $\vec{H}(t) = H_0(e^{-i\omega t} + c.c)\hat{z}$ with angular frequency ω applied along the z-axis. We consider the interaction between electrons, and describe the system in terms of a Hamiltonian. The expression consists of four parts, i.e., orbital energy, electronic Zeeman term, electron spin, and the hyperfine coupling, and is denoted as $H = H_\Delta + H_{eZ} + H_S + H_{hf}$. Additionally, the orbital energy of approximately 10^5 cm⁻¹ consists of four parts, i.e., $H_\Delta = H_K + H_e + H_{ee} + H_{so}$, where H_K, H_e, H_{ee}, and H_{SO} are the kinetic energy, Coulomb energy, energy of the Coulomb electrostatic interaction of the electrons of the ion, and spin-orbit coupling, respectively. The Mn²⁺ ion having the electron configuration 3d⁵ is a s-state ion with $S = 5/2$ and a ground level of $^6S_{5/2}$. When this ion is embedded in a crystal, the spin is affected by the crystal field produced by the neighboring ions because the 3d shell of the Mn²⁺ ion is the outermost one. We consider the EPR spectra at temperatures low enough such that the dynamic process is too slow to affect the EPRLP. Therefore, in the static region, the effective Mn²⁺ ground state manifold of a spin can be described by the spin Hamiltonian that contains zero-field-splitting terms

for an axial crystal field of the $^6S_{5/2}$ ground state. It can be expressed as

$$H_{sp} = H_{eZ} + H_{ZFS} + H_{hf} = \mu_B \vec{B} \cdot \vec{\vec{g}} \cdot \vec{S} + \sum B_k^q O_k^q + \vec{S} \cdot \vec{\vec{A}} \cdot \vec{I}, \quad (1)$$

where $\vec{B}$ is the applied static magnetic field, $\vec{\vec{g}}$ is the spectroscopic splitting tensor, $\vec{S}$ is the electron spin operator, B_k^q denotes a ZFS parameter (*k* rank, *q* component) associated with the extended Stevens operator O_k^q, $\vec{I}$ is the nuclear spin operator, and *A* is the hyperfine splitting constant. The ZFS Hamiltonian, in terms of the extended Stevens operators for the electron spin $S = 5/2$, has the following explicit form when the z-axis is parallel to the c-axis:

$$H_{ZFS} = \sum_{q=-2}^{+2} B_2^q O_2^q + \sum_{q=-4}^{+4} B_4^q O_4^q = B_2^0 O_2^0 + B_4^0 O_4^0 + B_4^3 O_4^3, \quad (2)$$

$$O_2^0 = 3S_z^2 - S(S+1) \quad (3)$$

$$O_4^0 = 35S_z^4 - 30S(S+1)S_z^2 + 25S_z^2 - 6S(S+1) + 3S^2(S+1)^2, \quad (4)$$

$$O_4^3 = \{S_z(S_+^3 + S_-^3) + (S_+^3 + S_-^3)S_z\}/4. \quad (5)$$

The EPRLW is calculated to be axially symmetric about the z-axis and analyzed in terms of the spin Hamiltonian with the parameters $g = 1.9920$, $B_2^0 = 7.2 \times 10^{-1}$ hGHz, $B_4^0 = -5 \times 10^{-5}$ hGHz, $B_4^3 = 4.7 \times 10^{-2}$ hGHz, and $A = 2.3 \times 10^{-1}$ hGHz ($A \ll g_e\mu_B B$) [7-9]. For a d⁵ ion in an octahedral crystal field having a small axial distortion, the $\vec{\vec{g}}$ and $\vec{\vec{A}}$ tensors can be considered approximately isotropic, within the experimental accuracy. Some authors have attempted to calculate the anisotropy of the g-factor, which is very small [9]. It was observed that it increases at low temperatures. More recently, the anisotropy of the *A* was simulated, but it did not resulting any significant improvement in the analysis of the Mn²⁺ spectrum. We obtain the analytical eigenenergies

$$\varepsilon_{\pm 5/2} = \pm g\mu_B B_z + B_2^0 + 90B_4^0 \\ + \sqrt{\left[\left(\pm \tfrac{3}{2}g\mu_B B_z + 9B_2^0 - 90B_4^0\right) + 90(B_4^3)^2\right]} + \tfrac{5}{4}A,$$

$$\varepsilon_{\pm 3/2} = \pm \tfrac{3}{2}g\mu_B B_z - B_2^0 - 180B_4^0 + \tfrac{3}{4}A,$$

$$\varepsilon_{\pm 1/2} = \mp g\mu_B B_z + B_2^0 + 90B_4^0 \\ - \sqrt{\left[\left(\mp \tfrac{3}{2}g\mu_B B_z + 9B_2^0 - 30B_4^0\right) + 90(B_4^3)^2\right]} + \tfrac{1}{4}A, \quad (6)$$

The most important results of our analysis are listed as follows: (i) We observed six intense resonances corresponding to the central transitions and involving splitting of the six central resonances that increases with an increase in the magnetic field strength. From these six
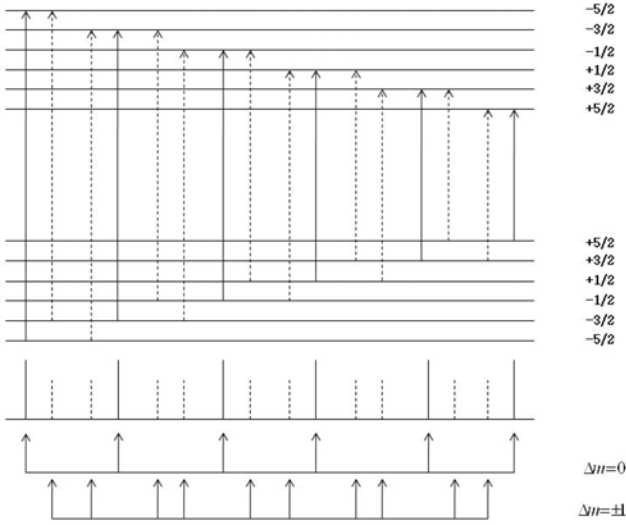
Fig. 1. Allowed transitions and forbidden transitions for a Mn^{2+} ion.

Fig. 2. (Color online) Specific heat as C_p *versus* T^3 in the temperature range 0.4-100 K.

strong absorptions are observed, corresponding to the $\langle -\frac{1}{2},\pm m| \rightarrow \langle +\frac{1}{2},\pm m|$ transitions. As algebraic sign of A is positive (according to the literature), the $m = -5/2$ component appears at low magnetic fields, whereas the $m = +5/2$ component appears at high fields. (ii) We observed a spreading of the other allowed transitions $|+\frac{3}{2},\pm m\rangle \rightarrow |+\frac{5}{2},\pm m\rangle$, $|+\frac{1}{2},\pm m\rangle \rightarrow |+\frac{3}{2},\pm m\rangle$, $|-\frac{3}{2},\pm m\rangle \rightarrow |-\frac{1}{2},\pm m\rangle$, and $|-\frac{5}{2},\pm m\rangle \rightarrow |-\frac{3}{2},\pm m\rangle$. (iii) Finally, we measured the allowed hyperfine transitions ($\Delta m = 0$) and five pairs of forbidden hyperfine transitions ($\Delta m = \pm 1$) in the EPR spectra of the Mn^{2+} ion, as illustrated in Fig. 1.

3. Specific Heat

The values of specific heats in the low-temperature region of a number of well-known ferroelectrics have been measured by mean of an adiabatic vacuum calorimeter. In LNO crystals, disorder is caused by the presence of impurities. The aim of this section is to measure low-temperature specific heat in the temperature range 0.4-100 K. The partition function for a LNO crystal doped with Mn^{2+} ions at 0.5 wt% was calculated using the energy levels in Eq. (6) as

$$Z = \frac{1}{2\pi i} \oint \frac{d\lambda}{\lambda^\alpha} \prod_{i \ge -5/2}\left(1 + \lambda e^{-\beta(\varepsilon_i - \mu B)}\right) \prod_{j \ge -5/2}\left(1 + \lambda e^{-\beta(\varepsilon_j + \mu B)}\right)$$
$$\times \prod_{k \le 0}\left(1 + \frac{1}{\lambda}e^{-\beta(\varepsilon_k + \mu B)}\right) \prod_{l \le 0}\left(1 + \frac{1}{\lambda}e^{-\beta(\varepsilon_l - \mu B)}\right) \quad (7)$$

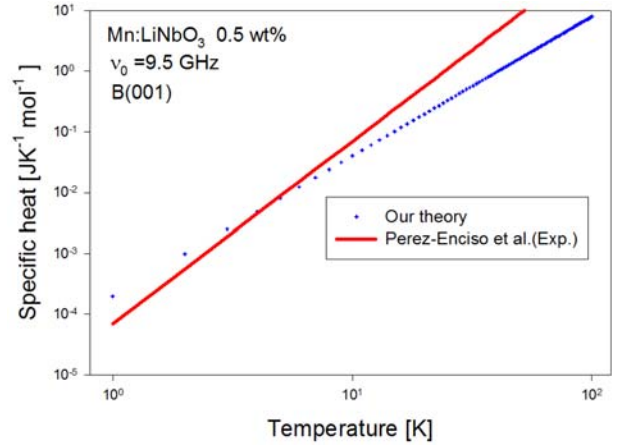where products with indices i and j represent excited electrons in the upper energy levels ($i, j > -5/2$), while those with k and l represent holes created at lower energy levels, and λ is simply a selector for the ground state $\beta \rightarrow \infty (T \rightarrow 0)$ that secures the number of electrons for arbitrary values of β and γ in the contour integral over the plane surrounding the origin. The free energy of a system is given by

$$F = -k_B T \sum_{\pm m} \langle \log Z \rangle_{EA} \quad (8)$$

where the $\langle \, \rangle_{EA}$ operator represents ensemble average of a system. The specific heat can be obtained from the free energy as

$$C_p = \frac{1}{k_B T^2} \frac{\partial^2}{\partial \beta^2} \langle \log Z \rangle_{EA}$$
$$= \frac{2k_B^2 T}{\varepsilon_{+m} - \varepsilon_{-m}} \int_0^\infty dx \, \log\left(1 + 4e^{-x} + e^{-2x}\right) + \frac{\pi^2 k_B^2 T}{3(\varepsilon_{+m} - \varepsilon_{-m})} \quad (9)$$
$$= 5.024 \frac{k_B^2 T}{\varepsilon_{+m} - \varepsilon_{-m}} + 3.290 \frac{k_B^2 T}{\varepsilon_{+m} - \varepsilon_{-m}},$$

Using the partition function in Eq. (7), the specific heat C_p of an LNO crystal was calculated in the range 0.4-100 K; Fig. 2 shows this plotted against T^3 and compared to the experimental data produced by E. Perez-Enciso *et al.* [20]. Our theoretical results follow a linear dependence to T^3, which suggests simple Debye behavior. Specific heat calculations show that the Debye temperature remains constant up to a large defect concentration, which contrasts with the large softening of elastic constants observed in glasses. These facts show the difficulty of producing a large distorted lattice in LNO crystals by means of substantial intrinsic disordering.

4. Line-profile Formula

Let $|+m\rangle$ be an eigenstate of H_Δ for a system in which the spin is up and $|-m\rangle$ be an eigenstate for a system in which the spin is down, with the same orbital. Then, the Schrödinger equation is expressed as $H_\Delta|+m\rangle = (E_\Delta \pm \hbar\omega_z/2)|\pm m\rangle$. We introduce the annihilation and creation operators, $a_{\pm m}$ and $a_{\pm m}^+$, for an eigenstate of H_Δ. We can express the commutator in terms of these operators, as shown below:

$$
\begin{aligned}
\left\langle [\sigma_-, \sigma_+(t)] \right\rangle_{EA} &= \left\langle \sum_{\pm m} \langle -m|\sigma_+(t)|+m\rangle \left\{ \left[\langle +m|\sigma_+(t)|+m\rangle \right. \right. \right. \\
&\quad \left. - \langle -m|\sigma_+(t)|-m\rangle \right] a_{-m}^+ a_{+m} \\
&\quad \left. \left. + \langle +m|\sigma_+(t)|-m\rangle \left(a_{-m}^+ a_{-m} - a_{+m}^+ a_{+m} \right) \right\} \right\rangle_{EA} \\
&= \sum_{\pm m} \langle -m|\sigma_-|+m\rangle \langle +m|\sigma_+(t)|-m\rangle \left[f(\varepsilon_{-m}) - f(\varepsilon_{+m}) \right],
\end{aligned}
$$

(10)

The spin matrices on the right hand side represent the electron operators in terms of the Heisenberg representation. We take into account only those terms in Eq. (10) that give a zero-order response line; the other terms are required only when a broad background study is essential. Thus, we will obtain the EPRLW. From Eq. (10) we can define the EPRLW, as shown below:

$$
\Lambda_{+-}^{epr}(\omega) \equiv \int_0^\infty \exp(-i\omega t) \langle +m|\sigma_+(t)|-m\rangle = \langle +m|R(\omega)|-m\rangle.
$$

(11)

There may be various methods for evaluating such a quantity that yields similar results; however, the evaluation is more effectively achieved using the PIT proposed by Argyres and Sigel, which is a method based on the equation of motion. Their theory seems to be quite general in the sense that it is based on rigorous formalism and the self-consistent projection technique. Thus we obtain the EPRLP function $\Gamma_{+-}^{epr}(\omega)$ is defined as follows:

$$
i\Gamma_{+-}^{epr}(\omega) = \frac{1}{(\sigma_+)_{+m-m}} \left\{ \left[\sum_{N=1}^\infty (L_{sp} G_\Delta(\omega) Q_{+-})^N L \right] \sigma_+ \right\}_{+m-m}
$$

(12)

In order to calculate Eq. (12), the propagator is expanded in a series expansion. The effective lowest-order approximation of the EPRLP function is given as follows:

$$
\begin{aligned}
\Gamma_{eff}^{epr}[\omega] &= \frac{1}{\hbar} \sum_{\mu \neq +m} \sum_{\Delta m \neq \pm 1} \frac{\varepsilon_{+m\mu}\varepsilon_{\mu+m}}{E_\Delta - \hbar\omega_z} \delta F_\mu + \frac{1}{\hbar} \sum_{\mu \neq -m} \sum_{\Delta m \neq \pm 1} \frac{\varepsilon_{-m\mu}\varepsilon_{\mu-m}}{E_\Delta + \hbar\omega_z} \delta F_\mu \\
&\quad + \frac{1}{\hbar} \sum_{\Delta m \neq \pm 1} \frac{2(E_\Delta + \hbar\omega)\varepsilon_{+m-m}^2}{\left[E_\Delta^2 - \hbar^2(\omega - \omega_z)^2 \right]} \delta F_\mu \left[1 - f(E_\Delta) \right] \\
&\quad + \frac{1}{\hbar} \sum_{\Delta m \neq \pm 1} \frac{2(E_\Delta + \hbar\omega)\varepsilon_{+m-m}^2}{\left[E_\Delta^2 + \hbar^2(\omega - \omega_z)^2 \right]} \delta F_\mu f(E_\Delta).
\end{aligned}
$$

(13)

The physical interpretation of Eq. (13) is as follows. The EPRLP terms represent the transition process of the electron spin from a state $+m(-m)$ to $-m(+m)$. Here, the distribution function represents as the condition for the transition process and $f(E_\Delta)[1-f(E_\Delta)]$ represents that for the transition $+m \rightarrow -m$. In Eq. (13), the distribution function can be written as $f(E_\Delta) = \exp[\beta(E_\Delta + \delta E) + 1]^{-1}$ for LNO crystal, the difference between the conduction band minimum and the Fermi energy is given by $\delta E = \varepsilon_g(T)/2 - \frac{3}{4} k_B T \ln(m_h/m)$. Here band gap is $\varepsilon_g(T) = \varepsilon_g(0) - \kappa T^2/(T + \xi)$, where κ and ξ are characteristic constants of the material. In order to compare the result with the experimental data of Ellabban et al., we adopt the following constants $m = 0.22\, m_0$, $m_h = 0.35\, m_0$, $s = 5.94 \times 10^5$ cm/s, $\varepsilon_g(0) = 6 \times 10^2$ cm^{-1}, $\kappa = 3.84$ cm^{-1}K^{-1}, and $\xi = 235$ K where m_0 is the free electron mass. Taking the frequency 9.5 GHz, which implies that angular frequency 5.97×10^{10} S^{-1}, and varying magnetic field B, we will calculate the EPRLW for various temperature. The EPR absorption power delivered to the system is given by

$$
P_{epr}(\omega) = \frac{1}{2} H_0^2 \, \mathrm{Re}\left[\chi_{+-}''(\omega) \right],
$$

(14)

where the absorption term is denoted by the Lorentzian. We consider the term $\Gamma_{+-}^{epr}(\omega) \equiv i S_{+-}^{epr}(\omega) + W_{+-}^{epr}(\omega)$, where the line-shift in EPR spectra is $S_{+-}^{epr}(\omega) = \mathrm{Im}[\Gamma_{+-}^{epr}(\omega)]$ and the EPR line-width is $W_{+-}^{epr}(\omega) = \mathrm{Re}[\Gamma_{+-}^{epr}(\omega)]$.

The PIT was applied to examine the temperature dependence of the EPRLW of the LNO crystal for magneto-optical quantum transitions. Through numerical calculations, we studied the dependence of absorption power on the magnetic field at different allowed transitions, as shown
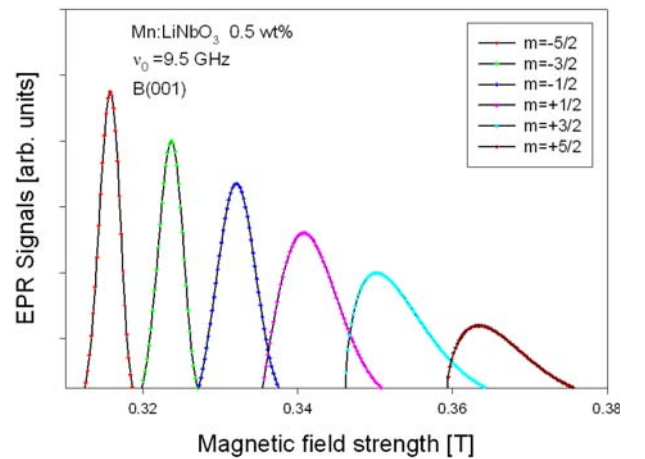

Fig. 3. (Color online) Magnetic field dependence of the EPR signals of the Mn^{2+} ion for allowed transition from $m = -5/2$ to $m = +5/2$. Hence, the $m = -5/2$ component appears at low magnetic fields and the $m = +5/2$ component appears at high fields.
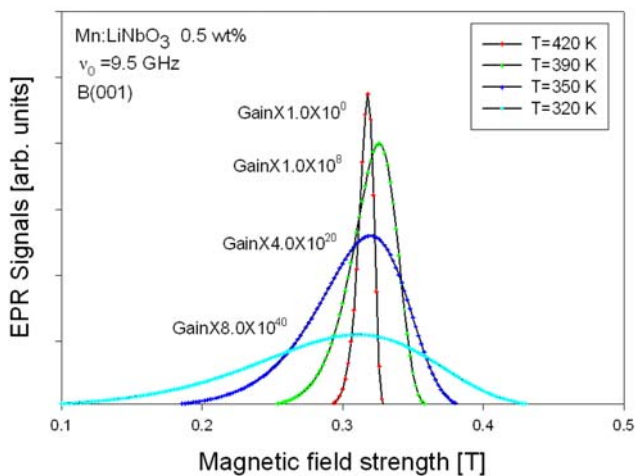
Fig. 4. (Color online) Magnetic field dependence of the EPR signals at T = 320, 350, 390, and 420 K with a frequency of 9.5 GHz.

in Fig. 3. The spectrum is inhomogeneous broadened by the magnetic dipole-dipole interaction. For concentrations of 0.5 wt% of Mn^{2+} ions, the hyperfine structure of six lines with a distance of approximately 9 mT is observed in this study. The orientation of Mn^{2+} ions broadens the hyperfine structure, with the broadening being greater towards the side of the spectrum that has a high magnetic field. In Fig. 4, we show the obtained magnetic field dependence of the absorption power, T = 320, 350, 390, and 420 K. The results are able to reasonable explain a motional narrowing. We can see from Fig. 5 that the EPRLW decreases exponentially as the temperature increases; that is, the temperature dependence in the range of 300-400 K obeys the Arrhenius behavior. This formula was used by
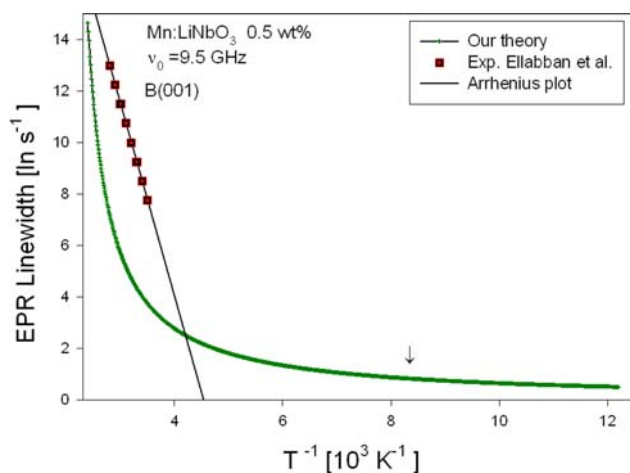

Fig. 5. (Color online) Reciprocal temperature dependence of the EPRLW of Mn^{2+} ion for transitions $+1/2 \leftrightarrow -1/2$ at a frequency of 9.5 GHz. The squares denote the experimental data of Ellabban *et al.*

us for the extraction of the relaxation time from the temperature dependence of narrowed EPR spectra line [15]. The result is shown in Fig. 5 as the dependence of the relaxation rate *versus* the reciprocal temperature. The EPRLW is barely affected in the low-temperature region because there is no correlation between the resonance fields and the distribution function. This kind of temperature behavior of the EPRLW indicates a motional narrowing of the spectrum, when Mn^{2+} impurity ions substitute the Nb^{5+} ions in an off-center position, and thus, there can be fast jumping of dipoles between several symmetrically equivalent configurations.

5. Conclusions

We have studied the various characteristics of ferroelectric LNO crystals doped with Mn^{2+} ions at 0.5 wt%, including specific heat and EPRLW; the latter was obtained using the PIT developed by Argyres and Sigel. It should be emphasized that using this PIT makes the analysis of magneto-optical quantum transitions in various circumstances much easier than is possible with other theories, as fewer steps are involved in the calculations. We discovered that specific heat follows a linear dependence on T^3, suggesting simple Debye behavior, and that the EPRLW decreases exponentially as the temperature increases; that is, the temperature dependence in the range of 300-420 K obeys Arrhenius behavior. If continued fraction methods [21, 22] are used in formulating the EPRLP function, improved numerical results may be obtained, and we plan to study such methods in the future.

Acknowledgment

References

[1] G. A. Samara, J. Phys: Condens. Matter **15**, R367 (2003).
[2] R. T. Smith and F. S. Welsh, J. Appl. Phys. **42**, 2219 (1971).
[3] D. B. Fraser and A. W. Warner, J. Appl. Phys. **37**, 3853 (1966).
[4] H. C. Huang, J. D. Knox, Z. Turski, R. Wargo, and J. J. Hanak, Appl. Phys. Lett. **24**, 109 (1974).
[5] F. R. Gfeller, Appl. Phys. Lett. **29**, 655 (1976).
[6] I. P. Kaminow, J. R. Carruthers, E. H. Turner, and L. W. Stulz, Appl. Phys. Lett. **22**, 540 (1973).
[7] T. Takeda, A. Watanabe, and K. Sugihara, Phys. Lett. A **27**, 14 (1968).
[8] M. P. Petrov, Fiz. Tver. Tela **10**, 3254 (1968).

[9] D. G. Rexford, Y. M. Kim, and H. S. Story, J. Chem. Phys. **52**, 860 (1970).

[10] S. Fujita and C. C. Chen, IJTP **2**, 59 (1969).

[11] H. Mori, Progr. Theor. Phys. **34**, 399 (1965).

[12] A. Suzuki and D. Dunn, Phys. Rev. B **25**, 7754 (1982).

[13] W. Xiaoguang, F. M. Peeters and J. T. Devreese, Phys. Rev. B **34**, 8800 (1986)

[14] X. Wu, F. M. Peeters, and J. T. Devreese, Phys. Rev. B **40**, 4090 (1989)

[15] X. J. Kong, C. W. Wei, and S. W. Gu, Phys. Rev. B **39**, 3230 (1989).

[16] P. N. Argyres and J. L. Sigel, Phys. Rev. Lett. **31**, 1397 (1973).

[17] J. I. Park, H. R. Lee, and S. H. Lee, Jpn. J. Appl. Phys. **51**, 52402 (2012)

[18] J. I. Park, J. Y. Sug, and H. R. Lee, J. Kor. Phys. Soc. **51**, 623 (2007)

[19] J. I. Park, J. Y. Sug, and H. R. Lee, J. Kor. Phys. Soc. **53**, 776 (2008)

[20] J. Y. Sug, Phys. Rev. B **64**, 235210 (2001)

[21] J. Y. Sug, Phys. Rev. E **55**, 314 (1997).

[22] J. I. Park, H. R. Lee, and H. K. Lee, J. Magnetics **16**, 108 (2011).

[23] R. Kubo, J. Phys. Soc. Jpn. **12**, 570 (1957).

[24] H. W. Goodwin and D. G. Seiler, Phys. Rev. B **27**, 3451 (1983).

[25] M. A. Ellabban, G. Mandula, and R. A. Rupp, SPIE **4607**, 327 (2002).

[26] E. Perez-Enciso and S. Vierira, Phys. Rev. B **57**, 13359 (1998).

[27] F. Lado, Phys. Rev. A **2**, 1467 (1970).

[28] T. Karasudani, K. Nagano, and H. Mori, Progr. Theor. Phys. **61**, 850 (1978).